

Attenuation of apoptosis in enterocytes by blocking potassium channels.

Anatoly Grishin¹, Henri Ford¹, Jin Wang¹, Hui Li²,

Vicenta Salvador-Recatala², Edwin Levitan² and Elena Zaks-Makhina².

¹Division of Pediatric Surgery, Children's Hospital of Los Angeles, Los Angeles, CA 90027 and

²Department of Pharmacology, University of Pittsburgh Medical School, Pittsburgh, PA, 15261.

Running head: blockade of K⁺ efflux arrests apoptosis in enterocytes

Address correspondence to:

Elena Zaks-Makhina,

Department of Pharmacology,

University of Pittsburgh,

200 Lothrop Street,

Pittsburgh, PA 15261,

Tel. 412-648-8693,

Fax 412-648-1945,

E-mail: elm59@pitt.edu.

Apoptosis plays an important role in maintaining the balance between proliferation and cell loss in the intestinal epithelium. Apoptosis rates may increase in intestinal pathologies such as inflammatory bowel disease and necrotizing enterocolitis, suggesting pharmacological prevention of apoptosis as a therapy for these conditions. Here we explore the feasibility of this approach using the rat epithelial cell line IEC-6 as a model. Based on the known role of K^+ efflux in apoptosis in various cell types, we hypothesized that K^+ efflux is essential for apoptosis in enterocytes and that pharmacological blockade of this efflux would inhibit apoptosis. Probing the intracellular $[K^+]$ with K^+ -sensitive fluorescent dye PBFI and measuring efflux of $^{86}Rb^+$, we have found that apoptosis-inducing treatment with the proteasome inhibitor MG-132 leads to two-fold increase in K^+ efflux from IEC-6 cells. Blockade of K^+ efflux with TEA, 4-AP, stromatoxin, chromanol 293B and the recently described K^+ channel inhibitor 48F10 prevents DNA fragmentation, caspase activation, release of cytochrome c from mitochondria, and loss of mitochondrial membrane potential. Thus, K^+ efflux occurs early in the apoptotic program and is required for the execution of the later events. Apoptotic K^+ efflux critically depends on activation of p38 MAP kinase. These results demonstrate for the first time the requirement of K^+ channel mediated K^+ efflux for progression of apoptosis in enterocytes and suggest the use of K^+ channel blockers to prevent apoptotic cell loss occurring in the intestinal pathologies.

Key words: IEC-6 cells, apoptotic K^+ efflux, p38 MAP kinase, intestinal pathologies.

In the intestinal epithelium, constant renewal of enterocytes is essential for maintaining tissue homeostasis. Epithelial stem cells in the intestinal crypts divide and differentiate into enterocytes that migrate to the villus tips where they ultimately undergo apoptosis (29). The balance between cell proliferation and cell loss in the crypts (11, 23, 39) and villi (19, 39) is controlled by apoptosis. Under pathologic conditions, the equilibrium between enterocyte proliferation and apoptosis may shift towards the latter process. Dysregulated or accelerated apoptosis as seen in several forms of inflammatory bowel disease (21), bowel injury (14) and infection (17, 35) may result in gut barrier failure. Thus, pharmacological manipulation or control of epithelial apoptosis may be a useful therapeutic modality for intestinal pathologies associated with excessive apoptosis.

Apoptosis is programmed cell death in response to extrinsic and intrinsic cues such as death receptor ligands or stresses. Although apoptosis is irreversible, its later steps such as caspase substrate cleavage, DNA fragmentation and dismantling of cellular structures can be prevented by blocking the earlier steps such as mitochondrial depolarization, cytochrome c release and activation of caspases. Recently, perturbations in ion homeostasis have been discovered as important steps in the apoptotic program (41). Dramatic efflux of K^+ ions occurs shortly after apoptotic stimulation and results in a significant decrease in intracellular $[K^+]$ (42). Importantly, blockade of K^+ efflux by elevated external $[K^+]$ or K^+ channel blockers prevents the later stages of apoptosis (27, 43, 37). These findings suggest that K^+ efflux via K^+ channels is an essential step of the apoptotic program that may present a valid target for pharmacological modulation of apoptosis. Involvement of K^+ currents in apoptosis has been demonstrated in neurons (26, 27, 42), lymphocytes (7, 13, 16), smooth muscle cells (5, 20), cardiac cells (6), and various cell lines (40), but not in enterocytes.

If K^+ currents are important for apoptotic processes in enterocytes, attenuation of apoptosis by K^+ channel block may be beneficial for treatment of intestinal disorders associated with increased enterocyte apoptosis. As a first step towards developing this therapeutic approach we examined whether the apoptotic insults evoke K^+ efflux, and whether blockade of K^+ efflux attenuates apoptosis in IEC-6 enterocytes. As a model cytoprotective drug we used 48F10 (3-bicyclo[2.2.1]hept-2-yl-benzene-1,2-diol), the compound that we identified previously as a K^+ channel blocker with high anti-apoptotic efficacy in neurons (45). In this study we demonstrate the importance of K^+ efflux for the progression of apoptosis in IEC-6 enterocytes and the prevention of apoptotic cell loss by pharmacological blockade of K^+ channels.

Materials and Methods.

Cell culture. IEC-6 cells were purchased from ATCC (Rockville, MD). Cells were grown in DMEM (Bio-Whittaker, Walkersville, MD) with 4.5 g/L glucose and 0.02 glutamine, supplemented with 5% Fetal Bovine Serum (Bio-Whittaker), 0.1 U/ml insulin, 100 µg/ml penicillin/ 100 µg/ml streptomycin at 37⁰ C and 10% CO₂. Passages 17-27 were used. CHO cells were grown in the media of the same composition as above but without insulin. CHO cells were incubated at 37⁰ C and 5% CO₂.

Induction of apoptosis. Subconfluent cultures were treated with 5 µM MG-132 (Biomol, Plymouth Meeting, PA) in growth medium. For peroxynitrite treatment cells were washed with PBS and incubated for 15 min in 50 µM peroxynitrite (Alexis Biochemical, San Diego, CA) in PBS (155.17 mM NaCl, 2.97 mM Na₂HPO₄ 1.06 mM KH₂PO₄, pH 7.2) and then transferred to growth medium. Control cells were treated with equivalent amounts of DMSO or decomposed peroxynitrite. Cells were harvested 4-20 h post treatment.

Measurement of intracellular K⁺. Intracellular K⁺ content was assessed using the cell permeant acetoxymethyl ester derivative of K⁺ binding fluorescent indicator (AM-PBFI, Molecular Probes, Eugene, OR) as recommended by the manufacturer. Cells were grown in 10 cm Petri dishes with 5 µM MG-132 for 7 h, trypsinized, washed with PBS and resuspended in 1 ml of media containing 10 µM AM-PBFI for dye loading. AM-PBFI was prepared by mixing 10 mM AM-PBFI in DMSO with 25% Pluronic-127 (Molecular Probes) in DMSO. Prior to loading, cell density in all samples was measured using hemocytometer and equalized, if necessary, by dilution with PBS. Cells were incubated with dye-containing media for 1 h at 37⁰ C and 10% CO₂. Following loading, cells were washed twice with PBS, pelleted by centrifugation at 400 x

g and resuspended in 1 ml PBS. AM-PBFI fluorescence in samples was measured as emission in the 400-600 nm range following excitation at 340 and 380 nm on the RF-5301PC fluorometer (Shimadzu, Kyoto, Japan). Fluorescence associated with AM-PBFI bound to K^+ was determined according to the formula $F=(E_{340}-E_{340\text{auto}})/(E_{380}-E_{380\text{auto}})$, where E_{340} and E_{380} are peak emission at 340 and 380 nm excitation, and $E_{340\text{auto}}$ and $E_{380\text{ auto}}$ are the respective autofluorescences.

$^{86}\text{Rb}^+$ flux assay. Cells were grown to confluence and loaded with $^{86}\text{Rb}^+$ for 4 h during incubation with 1 $\mu\text{Ci}/\text{ml}$ $^{86}\text{RbCl}$ (Amersham Biosciences, Piscataway, NJ). During the $^{86}\text{Rb}^+$ loading, cells were induced to undergo apoptosis and analyzed for $^{86}\text{Rb}^+$ efflux 2 and 5 h after induction. Prior to $^{86}\text{Rb}^+$ measurements cells were washed three times with $^{86}\text{Rb}^+$ -free media. Media was collected at 0-2 h time points and amount of released $^{86}\text{Rb}^+$ was measured by scintillation counting. At 2 h, cells were lysed with 1% SDS and residual radioactivity in cells was determined.

Cell toxicity assay. Cell death was assessed visually at 40x magnification and using the lactate dehydrogenase (LDH)-based toxicity assay kit (Sigma-Aldrich, St. Louis, MO) according to manufacturer's instructions.

DNA fragmentation assay. Cells were grown in 10 cm Petri dishes. Ten hours following induction of apoptosis cells were lysed for 10 min on ice with the DNA ladder buffer (20 mM Tris pH 7.5, 10 mM EDTA, 100 mM NaCl and 0.5% Triton X-100). The lysate was cleared by centrifugation at 14,000 g for 10 min at 4° C. The supernatant was adjusted to 1% SDS and 20 $\mu\text{g}/\text{ml}$ proteinase K (Pierce Biotechnology, Rockford, IL) and incubated at 45° C for 4 h. The sample was extracted with phenol/chlorophorm, treated with RNase A (50 $\mu\text{g}/\text{ml}$) and precipitated with 2 volumes of ethyl alcohol. DNA was analyzed on 2% agarose gel stained with ethidium bromide.

Caspase activity assay. Cells with active caspases were detected 10 h after induction of apoptosis by staining with FAM-VAD-FMK (Cell Technology, Minneapolis, MN) according to the manufacturer's protocol. Percentage of FAM-VAD-FMK-positive cells was determined by fluorescent microscopy.

Mitochondrial depolarization assay. Cells were stained for depolarization of mitochondrial membrane 7 h after induction of apoptosis with BD MitoSensor Dye (BD Biosciences Clontech, Palo Alto, CA) and analyzed by fluorescence microscopy as recommended by the manufacturer.

Cytochrome c release assay. Seven hours after induction of apoptosis, cells were harvested by centrifugation at 400 x g and washed with PBS. Cells were resuspended in 0.25 M sucrose, 10 mM HEPES pH 7.4, 1 mM EGTA with protease inhibitors (Pierce Biotechnology, Rockford, IL) and homogenized in 2-ml Dounce homogenizer with 40 strokes on ice. Nuclei were pelleted from homogenate by centrifugation at 1000x g and the supernatant was subjected to centrifugation at 20,000 x g for 1 h to pellet mitochondria. Mitochondrial pellets were resuspended in the initial volume of the lysis buffer. Equal volumes of the cytosolic fraction and mitochondria suspension were analyzed by Western blotting.

RT-PCR. Total RNA was isolated from IEC-6 cells using RNAqueous-4PCR Kit (Ambion, Austin, TX) and reverse transcribed with Superscript One-Step RT-PCR kit (Invitrogen, Carlsbad, CA) and oligo-dT primers. First strand cDNA was subjected to 30 cycles of PCR amplification with primers: for KvLQT1 5'-CAC CAA CAC CCC TCT GCC C-3' (forward) and 5'-GGG CTG AGG GTG GAA ACC CC-3' (reverse) (4), and for Kv2.1 5'-ACACCATCACCATCTCTCAAGG-3' (forward) and 5'-CTAAATTGTCAGCTCACCCCGA-3' (30). Product sizes are 229 bp and 269 bp, respectively. PCR products were analyzed by agarose gel electrophoresis and verified by sequencing.

Electrophysiology. Plasmids expressing Kv2.1 and KvLQT1-minK channels were transiently transfected into CHO cells using Lipofectamine reagent (Invitrogen). Construct KvLQT1-minK is a genetic fusion of the pore-forming subunit KvLQT1 and auxiliary subunit minK (a gift from Dr. Robert Kass). Green fluorescent protein (GFP) was used for co-transfection with Kv channels as a marker. 24-48 hours after transfection, cells exhibiting green fluorescence were used for whole-cell current recordings. In all cases, pipette solution contained 130 mM KCl, 10 mM HEPES, 4 mM MgCl₂, 10 mM EGTA and 1mM CaCl₂, pH 7.2. The bath solution contained 140 mM NaCl, 5.4 mM KCl, 10 mM HEPES, 1.8 mM CaCl₂, and 0.8 mM MgCl₂, pH 7.4. Test drugs were delivered using gravity-fed perfusion system. Data acquisition was performed with the Pulse-PulseFit software (HEKA Elektronik, Lambrecht, Germany).

Antibodies. Antibodies against cytochrome c (PharMingen, San Diego, CA), caspase-3 (Stressgen, San Diego, CA), p38 MAP kinase and phosphorylated p38 (Cell Signaling Technology, Beverly, MA) were used for Western blotting as directed by their manufacturers. Secondary horseradish peroxidase-conjugated antibodies were purchased from Bio-Rad Laboratories, Hercules, CA.

Chemicals. K⁺ channel blocker 48F10 (3-bicyclo[2.2.1]hept-2-yl-benzene-1,2-diol, ID# 5115671) was purchased from ChemBridge Corporation (San Diego, CA). Chromanol 293B was purchased from Sigma-Aldrich, St. Louis, MO; stromatoxin – from Alomone Labs, Jerusalem, Israel; SB202180 – from Calbiochem, San Diego, CA.

RESULTS.

Inducers of apoptosis cause K⁺ efflux in IEC-6 cells. An increase in K⁺ efflux has been identified as an essential early step of apoptosis in several tissues and cell lines. To examine whether K⁺ efflux occurs during the apoptosis in enterocytes, we measured K⁺ efflux in the IEC-6 rat intestinal epithelial cell line following apoptosis-inducing treatment. The IEC-6 cell line was chosen because it is a non-transformed primary enterocyte cell line that is likely to possess the wild type complement of all apoptotic genes. Logarithmically growing IEC-6 cells were treated with the proteasome inhibitor MG-132, which induces apoptosis via protein denaturing stress. Levels of intracellular K⁺ were measured 6 h following treatment using the K⁺ sensitive fluorescent dye PBFI. Figure 1A,B shows that cells treated with MG-132 retain less K⁺ than control cells. The loss of intracellular K⁺ was inhibited if the K⁺ channel inhibitor 48F10 was present in the media during treatment with MG-132 (Fig. 1A,B). To corroborate the data obtained with the PBFI dye and to determine the time course of K⁺ efflux, we used the ⁸⁶Rb⁺ flux assay that is based on the similar selectivity of K⁺ channels towards K⁺ and Rb⁺. Cells were pre-loaded with ⁸⁶Rb⁺ and the efflux of radioactivity was measured 2 h and 5 h following treatment with MG-132 (Fig. 1C,D). As shown in Figure 1D, ⁸⁶Rb⁺ efflux was similar in MG-132-treated and control cells 2 h following treatment. However, at 5 h, ⁸⁶Rb⁺ efflux occurred faster from MG-132-treated cells (Fig. 1C,D). 48F10 at 10 μM significantly reduced ⁸⁶Rb⁺ efflux evoked by MG-132 (Fig. 1C,D). ⁸⁶Rb⁺ efflux in control cells was insensitive to 48F10 at 10 μM (Fig. 1C,D) and 50 μM (not shown). These data indicate that treatment of IEC-6 cells with the apoptosis-inducing agent MG-132 leads to K⁺ efflux via 48F10-sensitive K⁺ channels.

Blockade of K⁺ efflux has cytoprotective effect. K⁺ efflux following treatment with an inducer of apoptosis may be an early step in the apoptotic process. Alternatively, it may be a consequence of apoptosis or cell damage. To distinguish between these two possibilities, we examined effects of blocking K⁺ efflux with 48F10 on cell death and apoptosis. Cell death was assessed visually as cell shrinkage and detachment as well as by lactate dehydrogenase release, a consequence of plasma membrane rupture. Apoptosis was assessed by internucleosomal DNA fragmentation. Figure 2A shows that 48F10 reduces cell death upon treatment with peroxyxynitrite. Similar results were obtained when apoptosis was induced by MG-132 (not shown). In the presence of 48F10, both LDH release and DNA fragmentation were significantly attenuated in cells treated to undergo apoptosis (Fig. 2B,C). These data argue that K⁺ efflux is a prerequisite and not a consequence of cell death following apoptosis-inducing treatments.

Blockade of K⁺ efflux stops apoptotic program at its early steps. The fact that K⁺ efflux blockade prevents DNA fragmentation, a late step of apoptosis, may indicate that lowering intracellular K⁺ concentration is required for the progression of apoptosis at this or earlier stage. To identify the stage of apoptosis requiring K⁺ efflux we examined whether execution of various events of the apoptotic program, including caspase activation, cytochrome c release from mitochondria, and changes in mitochondrial membrane potential, can be blocked by the K⁺ current inhibitor.

Activation of caspases (apoptotic proteases) was assayed using the fluorescent pan-caspase inhibitor FAM-VAD-FMK. This agent binds to mature active caspases but not to their precursors. Figure 3A shows that MG-132 dramatically increases the fraction of FAM-VAD-FMK positive cells 12 h post treatment, indicating caspase activation. 48F10 attenuated this effect in a concentration-dependent manner (Fig. 3B). At 10 μ M 48F10 reduced the frequency

of apoptotic cells to near background level. 48F10 did not interfere with FAM-VAD-FMK staining because it did not reduce the percentage of positive cells when added simultaneously with FAM-VAD-FMK (data not shown). Similar results were obtained when MG-132-induced K^+ efflux was prevented by other inhibitors of K^+ currents, including tetraethylammonium (TEA), 4-aminopyridine (4-AP) and elevated external $[K^+]$ (Fig. 3C). Effect of K^+ current blockade on caspase activation was also examined by Western blotting with the antibody that recognizes both active caspase-3 (15 kD) and its inactive precursor (25 kD) (Fig. 4). 48F10 inhibited caspase-3 activation by MG-132 in a concentration-dependent manner (Fig. 4A,B). 48F10 also inhibited caspase-3 activation by peroxynitrite (Fig. 4C,D). These results indicate that the blockade of K^+ efflux inhibits apoptosis at a stage upstream of caspase activation.

We next examined effects of 48F10 on cytochrome c release from mitochondria, an event in the apoptotic cascade that occurs prior to caspase activation. Treatment with MG-132 caused the release of cytochrome c from mitochondria into cytosol (Fig. 5A). Twelve hours post treatment, about 80 % of cytochrome c partitioned into the cytosol, compared to less than 5% in control cells. In the presence of 48F10 only about 10% of cytochrome c became cytosolic following MG-132 treatment. These data indicate that K^+ efflux occurs prior to the release of cytochrome c from mitochondria.

Release of cytochrome c occurs after the loss of mitochondrial membrane potential. To test whether the blockade of K^+ efflux prevents de-energization of mitochondria, we assessed changes in mitochondrial membrane potential using the fluorescent Mitosensor dye. This dye accumulates in energized, but not de-energized mitochondria. Treatment with MG-132 caused significant decrease in the fraction of cells displaying fluorescent mitochondria, which is

indicative of apoptosis (Fig. 5B). 48F10 reversed this effect (Fig. 5B). This result indicates that K^+ efflux occurs before the loss of mitochondrial membrane potential.

Apoptotic K^+ efflux is mediated by voltage-gated K^+ channels. The fact that 48F10 and TEA, the known blockers of Kv2.1 and KvLQT1 channels (12), prevent MG-132-induced apoptosis may indicate that these channels are involved in the apoptotic K^+ loss in IEC-6 cells. Kv2.1 and KvLQT1 channels are expressed in MG-132-treated IEC-6 cells at the mRNA level, as judged by RT-PCR (Fig. 6A). To further examine roles of these channels in apoptotic K^+ efflux, we tested anti-apoptotic effects of stromatoxin and chromanol 293B that have been reported to specifically inhibit Kv2.1 and KvLQT1, respectively (31, 9). Both inhibitors decreased percentage of cells with active caspases following treatment with MG-132, supporting the roles of Kv2.1 and KvLQT1 in apoptosis (Fig. 6B). Moreover, stromatoxin at 40 nM and chromanol 293B at 20 μ M concentration decreased frequency of cells with de-energized mitochondria by half, as judged by MitoSensor staining (not shown). In control experiments, we tested selectivity of 48F10, chromanol 293B and stromatoxin towards Kv2.1 and KvLQT1 currents in transfected CHO cells. Figure 6C shows that chromanol 293B inhibits both KvLQT1 and Kv2.1 currents, whereas stromatoxin affects Kv2.1 only. Taken together, these data point to Kv2.1 channel as a mediator of apoptotic K^+ efflux in IEC-6 cells, but do not exclude involvement KvLQT1 channel.

p38 MAP kinase is implicated in activation of apoptotic K^+ efflux. Based on the known role of p38 MAP kinase in apoptotic response various cell types (1, 24, 34, 36), we hypothesized that p38 is involved in regulation of apoptotic K^+ efflux in enterocytes. As shown in Figure 7A, MG-132 treatment leads to p38 activation appearing at 45 min and steadily increasing afterwards, consistent with p38 involvement in the apoptotic response. Pre-treatment with the specific p38

inhibitor SB202180 prevents proteolytic cleavage of procaspase-3 (Figure 7B) and decreases frequency of cells with active caspases (Fig. 7C) and frequency of cells with de-energized mitochondria (not shown) in cells treated with MG-132. Thus, progression of MG-132-induced apoptosis to the caspase activation step critically depends on p38 activity. To examine whether p38 activation is required for apoptotic K^+ efflux we measured release of $^{86}Rb^+$ by apoptotic cells in the presence or absence of the p38 inhibitor. Figure 8 shows that SB202180 significantly decreases efflux of $^{86}Rb^+$ following MG-132 treatment. This result points to p38 involvement in apoptotic activation of K^+ efflux in enterocytes.

DISCUSSION.

In this report we demonstrate that apoptosis in IEC-6 enterocytes is associated with the efflux of intracellular K^+ via K^+ channels. Because apoptosis does not occur, or is significantly attenuated following treatment with inhibitors of K^+ currents, the K^+ efflux is an essential step in the apoptotic process. Our data indicate that K^+ efflux is required for all the manifestations of apoptosis that we examined including DNA laddering, caspase activation, release of cytochrome c from mitochondria and loss of mitochondrial membrane potential. Therefore, K^+ loss may be one of the earliest events in the apoptotic program. The requirement of K^+ efflux for apoptosis has been previously demonstrated in other cell types, namely neurons (42), lymphocytes (7, 13, 16), cardiomyocytes (6), and smooth muscle cells (20). Our results demonstrate for the first time the critical requirement of K^+ efflux for apoptosis in enterocytes. We also show that in enterocytes both the apoptosis-specific K^+ efflux and apoptosis itself can be prevented by the specific pharmacological inhibitor of K^+ channels 48F10.

Our study shows that K^+ efflux is required for intrinsic, or mitochondrial type of apoptosis. This type of programmed cell death occurs following injury by stresses such as DNA damage, protein denaturing and oxidative stress. Treatment with MG-132 and peroxynitrite are examples of such stresses. The hallmark of intrinsic apoptosis is the loss of mitochondrial membrane potential with subsequent release of cytochrome c and other apoptotic factors from mitochondria into the cytosol, and subsequent caspase activation. At this point we do not know whether K^+ efflux also plays a role in extrinsic, or receptor-mediated apoptosis in enterocytes. Because enterocytes may express death receptors such as CD95/FAS (33) it is possible that K^+

efflux is also involved in the extrinsic pathway of apoptosis in enterocytes, as it was demonstrated for FAS-mediated apoptosis in lymphocytes (32).

The most intriguing question about the role of K^+ currents in apoptosis is how apoptotic stimuli evoke K^+ efflux. Our data demonstrate that apoptotic surge of K^+ efflux in enterocytes depends on the p38 MAPK signaling pathway. p38 is strongly activated by MG-132 in IEC-6 cells. Other apoptosis-inducing stresses including DNA damage, oxidative stress, and osmotic shock also activate p38 in enterocytes (data not shown). p38 activity is required for progression of apoptosis (as judged by caspase activation and de-energization of mitochondria) as well as for efficient apoptotic K^+ efflux. These data support the role of p38 in the apoptotic response to stresses and associated K^+ efflux. Our finding of p38 mediating the apoptotic K^+ efflux in enterocytes agrees with the known role of p38 in apoptosis in various cell types including enterocytes (1, 34, 36). Moreover, p38 has been previously implicated in the apoptotic K^+ current in neurons (24). It remains to be investigated whether activated p38 stimulates K^+ channel surface expression or affects biophysical properties of K^+ channels during apoptosis.

Before the mechanism of apoptotic K^+ current regulation can be tested, pro-apoptotic K^+ channels need to be identified. Our pharmacological data (Fig. 6) indirectly point to the voltage-gated channel Kv2.1 as a carrier of apoptotic K^+ efflux in IEC-6 cells. Indeed, apoptosis in IEC-6 cells is significantly attenuated in the presence of stromatoxin that specifically blocks Kv2.1 channel. However, we cannot exclude contribution of other K^+ channels, particularly KvLQT1 that strongly expresses in intestinal epithelia (38) and IEC-6 cells (Fig.6A). Indeed, TEA, 48F10 and chromanol 293B that inhibit KvLQT1 current exert strong anti-apoptotic effect in IEC-6 cells.

Our finding that the specific inhibitor of K⁺ channels 48F10 can prevent apoptosis in enterocytes may have an important clinical implication. Intestinal disorders such as ulcerative colitis (3, 15, 44), coeliac disease (2, 22, 25), necrotizing enterocolitis (18, 28) and microvillus inclusion disease (10) are associated with increased levels of enterocyte apoptosis. Specific inhibitors of enterocyte K⁺ channels may be useful in preventing or modulating gut barrier failure associated with these inflammatory conditions. 48F10 can be a prototype of such cytoprotective drugs. One of our future goals is to evaluate the efficacy of K⁺ channel blockers in the animal models of inflammatory bowel disease and necrotizing enterocolitis.

Footnotes.

Abbreviations: IEC, intestinal epithelial cells; CHO, Chinese hamster ovary; LDH, lactate dehydrogenase; TEA, tetraethylammonium; 4-AP, 4-aminopyridine; HEPES, N-2-hydroxyethylpiperazine-N'-2-ethanesulphonic acid; EGTA, ethylene glycol bis(2-aminoethyl ether)-N,N,N'N'-tetraacetic acid.

Acknowledgements.

We thank Dr. Colin Nichols and Dr. Ian Reynolds for using facilities in their laboratories, Dr. Robert Kass for KvLQT1-minK construct and Dr. Elias Aizenman for helpful discussion.

This work was supported by NIH NS048089 to EZM, NIH A1-494-73-01 to HR, NIH HL55312 to ESL and start-up Grant from Research Advisory Committee Children's Hospital of Pittsburgh to AG.

REFERENCES

1. Bossy-Wetzell E, Talantova MV, Lee WD, Scholzke MN, Harrop A, Mathews E, Gotz T, Han J, Ellisman MH, Perkins GA, Lipton SA. Crosstalk between nitric oxide and zinc pathways to neuronal cell death involving mitochondrial dysfunction and p38-activated K⁺ channels. *Neuron*, 41:351-65, 2004.
2. Ciccocioppo R, Di Sabatino A, Parroni R, Muzi P, D'Alo S, Ventura T, Pistoia MA, Cifone MG, Corazza GR. Increased enterocyte apoptosis and Fas-Fas ligand system in celiac disease. *Am J Clin Pathol* 115: 494-503, 2001.
3. D'Argenio G, Farrace MG, Cosenza V, De Ritis F, Della Valle N, Manguso F, Piacentini M. Expression of apoptosis-related proteins in rat with induced colitis. *Int J Colorectal Dis* 19: 451-60, 2004.
4. Demolombe S, Franco D, de Boer P, Kuperschmidt S, Roden D, Perea Y, Jarry A, Moorman AF, Escande D. Differential expression of KvLQT1 and its regulator IsK in mouse epithelia. *Am J Physiol Cell Physiol.*, 280:C359-72, 2001.
5. Ekhterae D, Platoshyn O, Krick S, Yu Y, McDaniel SS, Yuan JX. Bcl-2 decreases voltage-gated K⁺ channel activity and enhances survival in vascular smooth muscle cells. *Am J Physiol Cell Physiol* 281: C157-65, 2001.
6. Ekhterae D, Platoshyn O, Zhang S, Remillard CV, Yuan JX. Apoptosis repressor with caspase domain inhibits cardiomyocyte apoptosis by reducing K⁺ currents. *Am J Physiol Cell Physiol* 284: C1405-10, 2003.
7. Elliott JI, Higgins CF. IKCa1 activity is required for cell shrinkage, phosphatidylserine translocation and death in T lymphocyte apoptosis. *EMBO Rep* 4:189-94, 2003.
8. Fedida D, Maruoka ND, Lin S. Modulation of slow inactivation in human cardiac Kv1.5 channels by extra- and intracellular permeant cations. *J Physiol* 515: 315-29, 1999.
9. Gerlach U, Brendel J, Lang HJ, Paulus EF, Weidmann K, Bruggemann A, Busch AE, Suessbrich H, Bleich M, Greger R. Synthesis and activity of novel and selective I(Ks)-channel blockers. *J Med Chem.*, 44:3831-7, 2001.
10. Groisman GM, Sabo E, Meir A, Polak-Charcon S. Enterocyte apoptosis and proliferation are increased in microvillous inclusion disease (familial microvillous atrophy). *Hum Pathol* 31: 1404-10, 2000.
11. Hall PA, Coates PJ, Ansari B, Hopwood D. Regulation of cell number in the mammalian gastrointestinal tract: the importance of apoptosis. *J Cell Sci* 107: 3569-77, 1994.
12. Hadley JK, Noda M, Selyanko AA, Wood IC, Abogadie FC, Brown DA. Differential tetraethylammonium sensitivity of KCNQ1-4 potassium channels. *Br J Pharmacol.*, 129:413-5, 2000.
13. Hughes FM Jr, Bortner CD, Purdy GD, Cidlowski JA. Intracellular K⁺ suppresses the activation of apoptosis in lymphocytes. *J Biol Chem* 272: 30567-76, 1997.
14. Husain K D, Coopersmith CM. Role of intestinal epithelial apoptosis in survival. *Curr Opin Care* 9: 159-163, 2003.
15. Iwamoto M, Koji T, Makiyama K, Kobayashi N, Nakane PK. Apoptosis of crypt epithelial cells in ulcerative colitis. *J Pathol* 180: 152-9, 1996.

16. Jonas D, Walev I, Berger T, Liebetrau M, Palmer M, Bhakdi S. Novel path to apoptosis: small transmembrane pores created by staphylococcal alpha-toxin in T lymphocytes evoke internucleosomal DNA degradation. *Infect Immun* 62: 1304-12, 1994.
17. Jones NL, Islur A, Haq R, Mascarenhas M, Karmali MA, Perdue MH, Zanke BW, Sherman PM. Escherichia coli Shiga toxins induce apoptosis in epithelial cells that is regulated by the Bcl-2 family. *Am J Physiol Gastrointest Liver Physiol* 278: G811-9, 2000.
18. Kelly N, Friend K, Boyle P, Zhang XR, Wong C, Hackam DJ, Zamora R, Ford HR, Upperman JS. The role of the glutathione antioxidant system in gut barrier failure in a rodent model of experimental necrotizing enterocolitis. *Surgery* 136: 557-66, 2004.
19. Kitazawa H, Nishihara T, Nambu T, Nishizawa H, Iwaki M, Fukuhara A, Kitamura T, Matsuda M, Shimomura I. Intectin, a novel small intestine-specific glycosylphosphatidylinositol-anchored protein, accelerates apoptosis of intestinal epithelial cells. *J Biol Chem* 279: 42867-74, 2004.
20. Krick S, Platoshyn O, Sweeney M, Kim H, Yuan JX. Activation of K⁺ channels induces apoptosis in vascular smooth muscle cells. *Am J Physiol Cell Physiol* 280: C970-9, 2001.
21. Levine AD. Apoptosis: implications for inflammatory bowel disease. *Inflamm Bowel Dis* 6: 191-205, 2000.
22. Maiuri L, Ciacci C, Raia V, Vacca L, Ricciardelli I, Raimondi F, Auricchio S, Quaratino S, Londei M. FAS engagement drives apoptosis of enterocytes of coeliac patients. *Gut* 48: 418-2, 2001.
23. Marshman E, Ottewell PD, Potten CS, Watson AJ. Caspase activation during spontaneous and radiation-induced apoptosis in the murine intestine. *J Pathol* 195: 285-92, 2001.
24. McLaughlin B, Pal S, Tran MP, Parsons AA, Barone FC, Erhardt JA, Aizenman E. p38 activation is required upstream of potassium current enhancement and caspase cleavage in thiol oxidant-induced neuronal apoptosis. *J Neurosci.*, 21:3303-11, 2001.
25. Moss SF, Attia L, Scholes JV, Walters JR, Holt PR. Increased small intestinal apoptosis in celiac disease. *Gut* 39: 811-7, 1996.
26. Nadeau H, McKinney S, Anderson DJ, Lester HA. ROMK1 (Kir1.1) causes apoptosis and chronic silencing of hippocampal neurons. *J Neurophysiol* 84: 1062-75, 2000.
27. Pal S, Hartnett KA, Nerbonne JM, Levitan ES, Aizenman E. Mediation of neuronal apoptosis by Kv2.1-encoded potassium channels. *J Neurosci* 23:4798-802, 2003.
28. Potoka DA, Upperman JS, Nadler EP, Wong CT, Zhou X, Zhang XR, Ford HR. NF-kappaB inhibition enhances peroxynitrite-induced enterocyte apoptosis. *J Surg Res* 106: 7-14, 2002.
29. Potten CG. Epithelial cell growth and differentiation: intestinal apoptosis. *Am J Physiol* 273: G253-G257, 1997.
30. Rao JN, Platoshyn O, Li L, Guo X, Golovina VA, Yuan JX, Wang JY. Activation of K⁺ channels and increased migration of differentiated intestinal epithelial cells after wounding. *Am J Physiol Cell Physiol.*, 282:C885-98, 2002.
31. Shiau YS, Huang PT, Liou HH, Liaw YC, Shiau YY, Lou KL. Structural basis of binding and inhibition of novel tarantula toxins in mammalian voltage-dependent potassium channels. *Chem Res Toxicol.*, 16:1217-25, 2003.

32. Storey NM, Gomez-Angelats M, Bortner CD, Armstrong DL, Cidlowski JA. Stimulation of Kv1.3 potassium channels by death receptors during apoptosis in Jurkat T lymphocytes. *J Biol Chem* 278: 33319-26, 2003.
33. Strater J and Moller P. CD95(FAS/APO-1)/CD95L in the gastrointestinal tract: fictions and facts. *Virchows Arch* 442: 218-225, 2003.
34. Vachon PH, Harnois C, Grenier A, Dufour G, Bouchard V, Han J, Landry J, Beaulieu JF, Vezina A, Dydensborg AB, Gauthier R, Cote A, Drolet JF, Lareau F. Differentiation state-selective roles of p38 isoforms in human intestinal epithelial cell anoikis. *Gastroenterology*. 123(6):1980-91, 2002.
35. Wada Y, Mori K, Iwanaga T. Apoptosis of enterocytes induced by inoculation of a strain of attaching and effacing Escherichia coli and verotoxin. *J Vet Med Sci* 59: 815-8, 1997.
36. Wada T, Penninger JM. Mitogen-activated protein kinases in apoptosis regulation. *Oncogene*, 23:2838-49, 2004.
37. Wang X, Xiao AY, Ichinose T, Yu SP. Effects of tetraethylammonium analogs on apoptosis and membrane currents in cultured cortical neurons. *J Pharmacol Exp Ther* 295: 524-30, 2000.
38. Warth R, Barhanin J. Function of K⁺ channels in the intestinal epithelium. *J Membr Biol.*, 193:67-78, 2003.
39. Watson AJ, Pritchard DM. Lessons from genetically engineered animal models. VII. Apoptosis in intestinal epithelium: lessons from transgenic and knockout mice. *Am J Physiol Gastrointest Liver Physiol* 782: G1-5, 2000.
40. Yu SP. Regulation and critical role of potassium homeostasis in apoptosis. *Prog Neurobiol* 70: 363-86, 2003.
41. Yu SP, Canzoniero LM, Choi DW. Ion homeostasis and apoptosis. *Curr Opin Cell Biol* 13: 405-411, 2001.
42. Yu SP, Yeh CH, Sensi SL, Gwag BJ, Canzoniero LM, Farhangrazi ZS, Ying HS, Tian M, Dugan LL, Choi DW. Mediation of neuronal apoptosis by enhancement of outward potassium current. *Science* 278: 114-7, 1997.
43. Yu SP, Yeh CH, Gottron F, Wang X, Grabb MC, Choi DW. Role of the outward delayed rectifier K⁺ current in ceramide-induced caspase activation and apoptosis in cultured cortical neurons. *J Neurochem* 73: 933-41, 1999.
44. Yukawa M, Iizuka M, Horie Y, Yoneyama K, Shirasaka T, Itou H, Komatsu M, Fukushima T, Watanabe S. Systemic and local evidence of increased Fas-mediated apoptosis in ulcerative colitis. *Int J Colorectal Dis* 17: 70-6, 2002.
45. Zaks-Makhina E, Kim Y, Aizenman E, Levitan ES. Novel neuroprotective K⁺ channel inhibitor identified by high-throughput screening in yeast. *Mol Pharmacol* 65: 214-9, 2004.

FIGURE LEGENDS

Figure 1. Apoptotic inducer MG-132 evokes K^+ efflux via K^+ channels. A. Emission spectra of PBFI-loaded cells treated for 7 h with DMSO solvent (squares), 5 μ M MG-132 (triangles) and 5 μ M MG-132 plus 10 μ M 48F10 (circles). Open markers – spectra emitted by PBFI in complex with K^+ following excitation at 340 nm, filled markers – spectra of total PBFI in the same samples following excitation at 380 nm (control for dye loading), F – fluorescence intensity. B. Relative fluorescence of PBFI-loaded cells in the presence and absence of 10 μ M 48F10. Bars represent mean \pm s.e.m. fluorescence of MG-132 treated cells as percent of fluorescence of untreated cells ($n = 3$ experiments). Inset shows structural formula of 48F10. C. Time course of $^{86}\text{Rb}^+$ efflux. Cells were loaded with $^{86}\text{Rb}^+$ and treated with DMSO (filled squares), 5 μ M MG-132 (filled triangles), 5 μ M MG-132 plus 10 μ M 48F10 (open triangles), or 10 μ M 48F10 for 5 h. Cells were washed and $^{86}\text{Rb}^+$ release was measured at the indicated time points. D. $^{86}\text{Rb}^+$ efflux at 2 and 5 h following induction of apoptosis. Cells were loaded with $^{86}\text{Rb}^+$ and treated with 5 μ M MG-132 (gray bars) or 5 μ M MG-132 plus 10 μ M 48F10 (black bars) for 2 or 5 h. $^{86}\text{Rb}^+$ released from cells was measured 25 min after washing. Data shown are mean \pm s.e.m. of 3 independent experiments.

Figure 2. Blockade of K^+ efflux has cytoprotective effect. A. Photographs of cells treated with 50 μ M peroxynitrite for 7 h in the presence and absence of 10 μ M 48F10. Dead cells appear light and round. B. LDH release from control and cells treated by apoptosis inducers

in the presence and absence of 10 μM 48F10. Data presented as percentage of LDH release from untreated cells in the absence of 48F10. Bars represent mean \pm s.e.m. from 3 independent experiments. C. DNA fragmentation in cells treated for 12 h with 5 μM MG132 and 48F10 at the indicated concentrations.

Figure 3. Blockers of K^+ efflux decrease frequency of cells with active caspases. A. FAM-VAD-FMK fluorescence in control cells and cells treated for 10 h with 5 μM MG-132 in the presence and absence of 10 μM 48F10. B. Fraction of FAM-VAD-FMK-positive cells in untreated control and cultures treated for 10 h with 5 μM MG-132 at the indicated concentrations of 48F10. C. Fraction of FAM-VAD-FMK-positive cells in untreated control and cells treated with 5 μM MG-132 and the indicated concentrations (mM) of KCl, 4-AP and TEA. Bars in B and C represent mean \pm s.e.m. from 3 independent experiments.

Figure 4. Blockade of K^+ efflux prevents pro-caspase-3 cleavage. A. Western blot analysis of pro-caspase-3 cleavage in cells treated for 10 h with 5 μM MG132 in the presence of 48F10 at indicated concentrations. B. Quantification of experiment in A. Band densities were measured by densitometry and relative content of the 15 kD band was determined. C. Western blot analysis of pro-caspase-3 cleavage in cells treated with 50 μM peroxynitrite in the presence and absence of 10 μM 48F10. D. Quantification of experiment in C. Bars in B and D are mean \pm s.e.m., n=3 experiments.

Figure 5. Blockade of K^+ efflux prevents cytochrome c release and de-energization of mitochondria. A. Western blot analysis of cytochrome c release from mitochondria in cells

treated with 5 μ M MG-132 in the presence and absence of 10 μ M 48F10. M – mitochondrial fraction, C – cytosol. B. Analysis of mitochondrial membrane depolarization in control and treatment with 5 μ M MG-132 in the presence and absence of 10 μ M 48F10. Bars represent mean percentage \pm s.e.m. of cells with non-fluorescent mitochondria ($n > 300$ cells).

Figure 6. Identification of pro-apoptotic K^+ channels. A. Products of RT-PCR of total RNA from IEC-6 cells treated for 6 h with MG-132. Template was amplified by PCR with Kv2.1 and KvLQT1 primers. Identity of PCR products was verified by sequencing. B. Concentration-dependent inhibition of apoptosis by chromanol 293B and stromatoxin. Cells were treated with 5 μ M MG-132 for 10 h with or without inhibitors at the indicated concentrations, μ M for chromanol 293B and nM for stromatoxin. Apoptotic cells were scored by FAM-VAD-FMK fluorescence. Apoptosis efficiency is expressed relative to MG-132 treatment without inhibitors, which was assumed 100%. Bars are mean \pm s.e.m., $n = 3$ experiments. C. Representative whole-cell K^+ current recordings from CHO cells transfected with Kv2.1 and KvLQT1 cDNAs in the presence and absence of K^+ channel blockers. Concentrations of 48F10 and chromanol 293B are in μ M, stromatoxin is in nM. K^+ currents were elicited by pulses to +60 mV, delivered every 10 seconds, from a holding potential of -70 mV.

Figure 7. p38 MAPK mediates MG132-induced apoptosis. A. Time-dependent activation of p38 by MG-132. Cells were treated with 5 μ M MG-132 for indicated time (min). Activating phosphorylation of p38 was detected by Western blotting with phospho-specific antibody. The lower panel is reprobe of the same blot with regular p38 antibody. B. Specific inhibitor

of p38 blocks MG-132-induced pro-caspase-3 cleavage. IEC-6 cells were pre-treated with or without 20 μ M SB202180 for 20 min and then treated with MG-132 for 6 h. Caspase-3 cleavage was examined by Western blotting with anti-caspase-3 antibody. Active caspase appears as 15 kD band. C. Specific inhibitor of p38 attenuates MG-132-induced apoptosis. IEC-6 cells were pre-treated with or without 20 μ M SB202180 for 20 min and then treated with 5 μ M MG-132 for 12 h. Apoptosis was scored as percentage of FAM-VAD-FMK-positive cells. Bars are mean \pm s.e.m., n=3 experiments. *P value < 0.05.

Figure 8. p38 MAPK mediates apoptotic K⁺ efflux. A. Time course of ⁸⁶Rb⁺ efflux from MG-132-treated cells in the presence and absence of p38 inhibitor SB202180. IEC-6 cells were loaded with ⁸⁶Rb⁺ for 4h. Cells were then pre-treated with or without 20 μ M SB202180 for 20 min, and apoptosis was induced by treatment with 5 μ M MG-132 for 5 h. Cells were washed and ⁸⁶Rb⁺ release into medium at 0-80 min time points was measured by scintillation counting. B. Quantification of ⁸⁶Rb⁺ release at 80 min time point from three experiments. Bars are mean \pm s.e.m., n=3 experiments. *P value < 0.05.

Fig 1

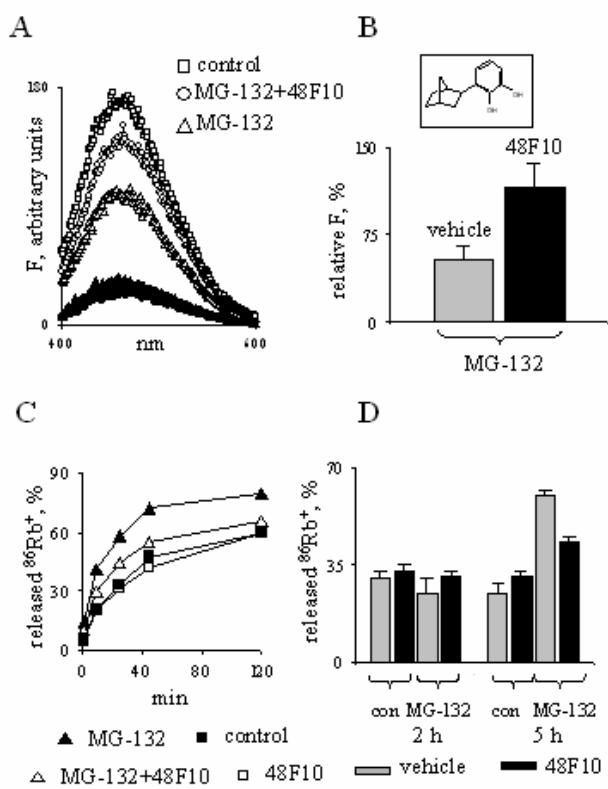


Fig. 2

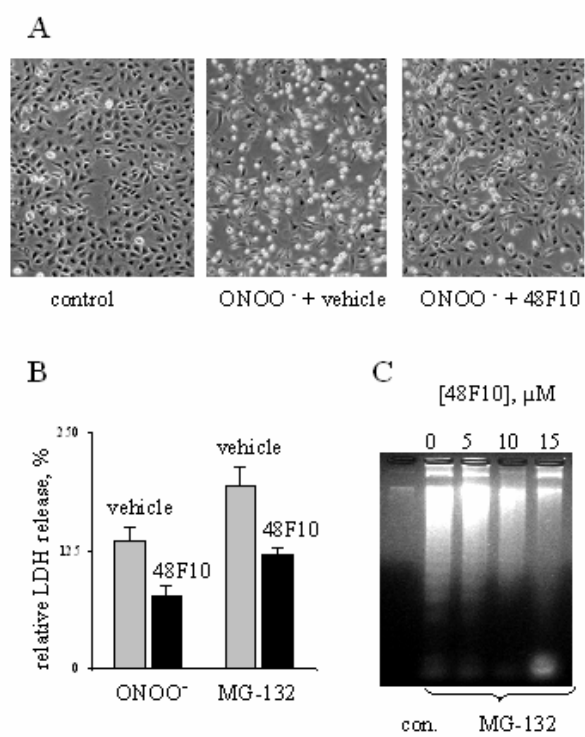


Fig 3

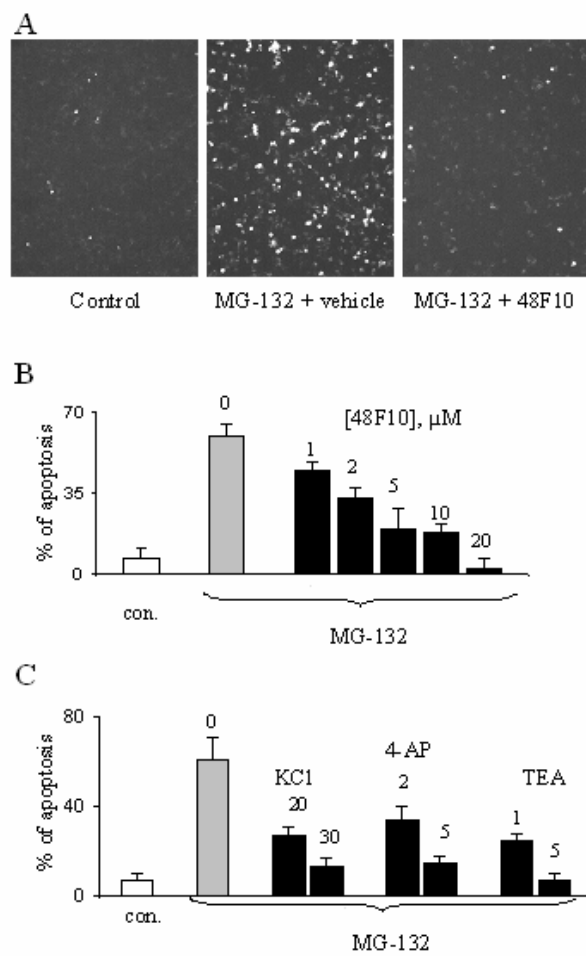


Fig 4

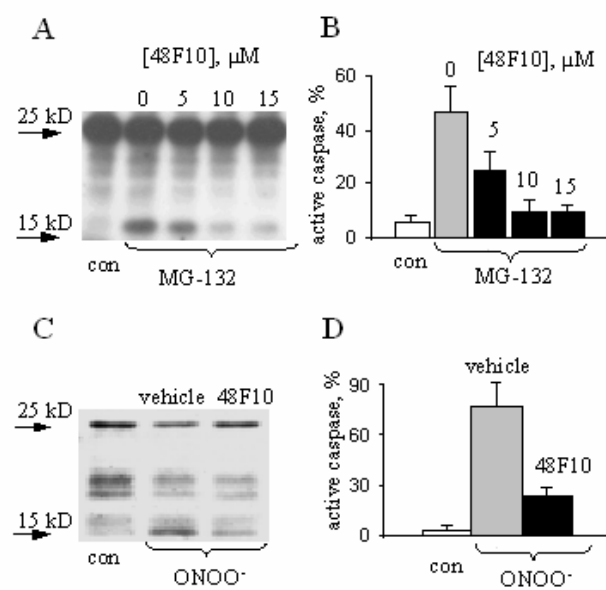


Fig 5

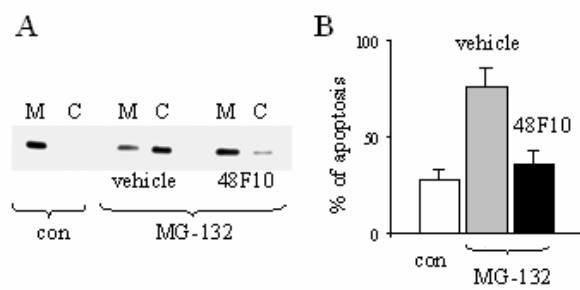


Fig. 6

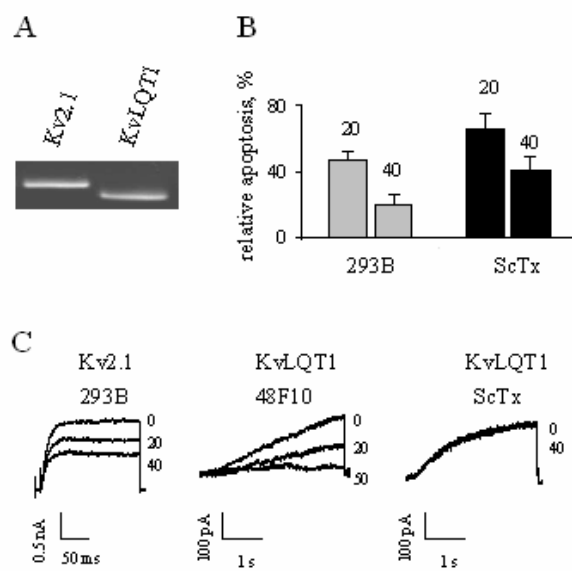


Fig. 7

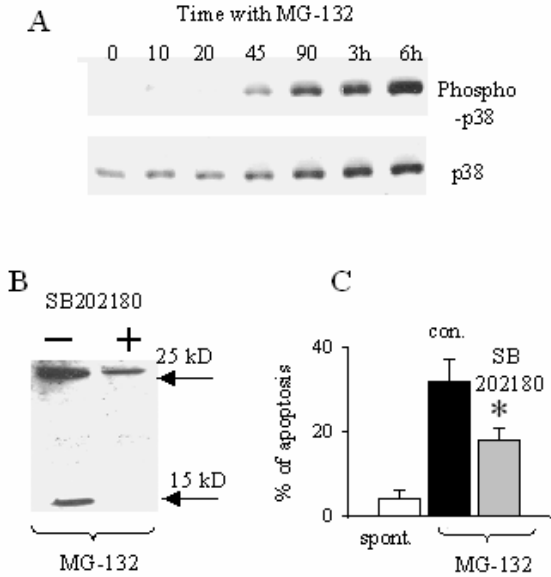


Fig. 8

